Experimental Constraints on Carbon Solubility in Terrestrial Magma Oceans: Implications for the Efficiency of Early Carbon Cycling on Earth and Mars. M. S. Duncan[1,2] and R. Dasgupta[1]; [1]Department of Earth Science, Rice University, Houston, TX, USA (Rajdeep.Dasgupta@rice.edu), [2]Geophysical Laboratory, Carnegie Institution for Science, Washington, D. C., USA (mduncan@carnegiescience.edu)

Introduction: For understanding of the evolution of the deep carbon cycle of terrestrial planets, we must first place constraints on the behavior of C during the early stages of planet formation, i.e., in the magma ocean (MO). Particularly, we must know the solubility of C in a MO composition, and the partitioning behavior between the MO, the early atmosphere, and the core [1,2]. Because these three reservoirs are linked during the early differentiation of planets, the C content of each reservoir are strongly influenced by the ability of the MO to dissolve C. For both the atmosphere–MO and core–MO partitioning, knowledge of the solubility of carbon at reducing conditions is critical, i.e., the solubility of C in MO at graphite/diamond saturation.

The solubility of C in silicate melt is primarily controlled by pressure (P), oxygen fugacity (fO_2), temperature (T), and silicate composition [3,4]. Carbon can dissolve in silicate melt as a variety of species, but at fO_2 relevant for near-core-forming conditions (IW-2 to IW+2) and during MO crystallization, the primary C species is thought to be carbonate (CO_3^{2-}) [3].

Current estimates of CO_2 solubility in depolymerized, ultramafic liquids derive from 1) experiments performed at fO_2 conditions several orders of magnitude higher than metal-present, core-forming conditions that measured bulk C contents of the quenched, ultramafic material [5]; and 2) extrapolated from CO_2 contents measured in mafic/basaltic compositions using a compositional parameter, such as NBO/T [6]. However, using only NBO/T may not reliably take into account the effects of different network modifiers, such as Ca^{2+} and Mg^{2+} on CO_2 solubility, because within mafic compositions NBO/T variation is tied mostly to variation of CaO, whereas extrapolation from mafic to ultramafic compositions requires a large increase of MgO content with little change in CaO. Therefore, in order to determine the behavior of C in a MO, it is critical to constrain the magnitude and the compositional controls on the solubility of CO_2 in ultramafic liquid under reducing conditions.

Experimental Methods: Piston cylinder experiments were conducted under nominally anhydrous conditions at graphite saturation to constrain the CO_2 content on a range of compositions from mafic toward the ultramafic compositional field. Experiments were at a fixed P (1.0 GPa), T (1600 °C), and logfO_2 (~ IW+1.6; measured using Pt-Fe alloy). We also conducted experiments with variable Ca and Mg but constant CaO+MgO to determine their relative effects on carbonate (CO_3^{2-}) dissolution in the silicate melts.

Experimental glass compositions were confirmed with electron microprobe analyses, and CO_3^{2-} contents were measured with Fourier Transform Infrared Spectroscopy (Fig. 1). CO_2 contents generally increased with increasing MgO content and NBO/T and decreasing Ca#. For the fixed CaO+MgO experiments, CO_2 contents increased with CaO content at a relatively constant NBO/T.

CO_2 Solubility Model: We used our experimental results to construct a compositional parameter that describes the effect of various silicate components on the CO_2 content in the melt:

$$[X] = aX_{CaO} + bX_{MgO} + cX_{FeO} + dX_{SiO_2} + eX_{Al_2O_3} \quad (1)$$

which can be combined with the thermodynamically-based equation of [4] that describes the effects of P, T, and fO_2 on carbonate dissolution via:

$$\log K' = \log K'(\text{Holloway}) + A*[X] + B \quad (2)$$

$$X_{CO_3^{2-}}^{melt} = \frac{\exp[2.303*(\log K' + \log fO_2)]}{\{1+\exp[2.303*(\log K' + \log fO_2)]\}} \quad (3)$$

We derived the a, b, c, d, e, A, and B coefficients using the least squares method, and the overall fit of the adjusted equation to our CO_2 data has an R^2 value of 0.871. With this model, we then determined the CO_2 content of ultramafic (MO) compositions at graphite saturation over a range of P, T, and fO_2 (Fig. 1). It is clear from Figure 1 that the peridotite liquid has a higher CO_2 solubility compared to those of basalts.

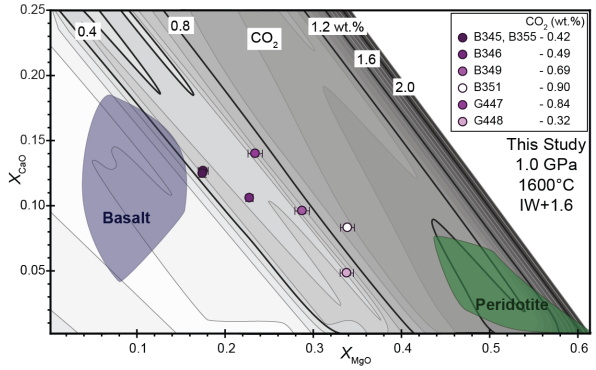

Figure 1. CO_2 solubility contours (0.1 wt.% intervals, darker shading indicating higher CO_2) at graphite saturation based on our model in mole fraction of MgO (X_{MgO}) versus mole fraction of CaO (X_{CaO}) space, at 1 GPa, 1600 ºC, and fO_2 of IW+1.6, conditions similar to our experiments. The compositions of our experimental glasses (circles) and the range of peridotites (green) and terrestrial basalts (blue) are plotted.

Application to Earth: In order to apply this model to a cooling MO, we used peridotite partial melting experiments [7] to estimate melt composition between the solidus and liquidus as a function of melt fraction (F), controlled by T, and P. The fO_2 of the system is controlled by the presence of a metallic phase, which will also control the valance state of Fe in the melt. Here, we have assumed that metal present at 5 GPa will set the fO_2 at IW [2]. From there, we can calculate the $Fe^{3+}/\Sigma Fe$ value in the melt [8], which we have assumed is constant as P decreases along an adiabat. This in turn sets the fO_2 of the melt, which decreases to between IW-1 and IW-1.5 as P and T decrease to the surface.

As the MO cools, C solubility drops and the C once dissolved in the liquid will precipitate out as graphite or diamond. As an example, if the bulk C content of the MO is 1000 ppm, we can calculate the amount of C precipitated as the MO cools (Fig. 2). For an adiabat that begins at the surface slightly below the liquidus (T_P = 1700 °C), the CO_2 solubility of the melt increases with depth by ~120% from ~40 pmm. This means that any graphite that is precipitated in the melt at the surface due to the cooling of the MO will redissolve into the silicate melt as convection carries it deeper.

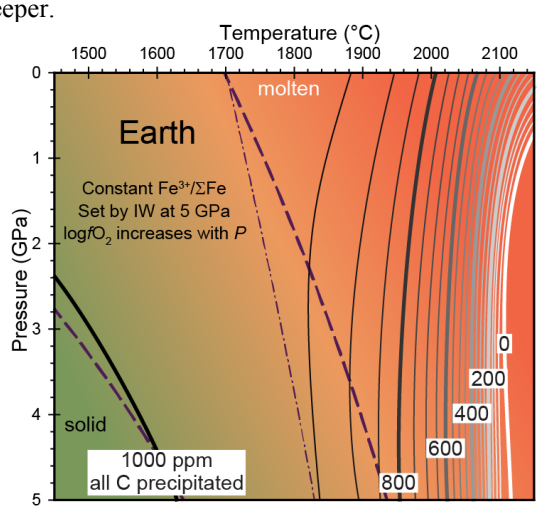

Figure 2. Contours of graphite precipitation (solid lines, 50 ppm intervals) of a cooling MO with a bulk C content of 1000 ppm. Based on calculated CO_2 contents of our model along P-T paths of MO adiabats (dash-dot line) with an fO_2 path decreasing upward from IW at 5 GPa. Also shown are the peridotite solidus [9] and liquidus [10] (dashed lines). Background shading denotes T (a proxy for F) where green indicates a completely solid mantle (F=0) and dark orange is a completely molten mantle (F=100). Contour colors denote amount of graphite precipitated with white indicating all carbon is dissolved as CO_3^{2-} in the peridotite, to black indicating all carbon is precipitated graphite.

Application to Mars: Similar to the Earth, we used bulk Mars partial melting experiments [11,12] to estimate melt composition after dropping below the liquidus as a function of melt fraction (F), controlled by T, and P. We followed the same procedure to determine fO_2, and applied our model to determine the C solubility of a martian MO. Overall, the C solubility dropped by an order of magnitude, likely due to the high Fe content of the martian compositions relative to the experimental compositions.

For the martian example, we used a bulk C content of 100 ppm to calculate the amount of C precipitated as the MO cools (Fig. 3). For an adiabat below the liquidus with a T_P = 1600 °C, the solubility of CO_2 in the melt increases by ~165% with depth. So for Mars, as for Earth, graphite precipitated at the surface with redissolved into the MO if carried deeper.

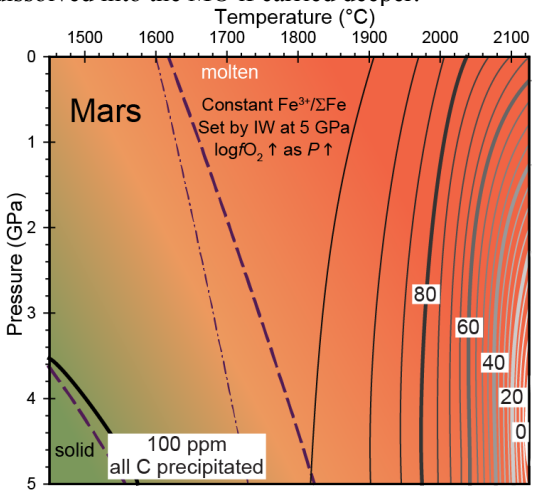

Figure 3. Contours of graphite precipitation (5 ppm intervals) of a cooling MO with a bulk C content of 100 ppm. Based on our model CO_2 contents along P-T paths of MO adiabats (dash-dot line) and an fO_2 path decreasing upward from IW at 5 GPa. Also shown are estimated martian solidus and liquidus (dashed lines). Background shading and contour colors as in Figure 2.

Conclusions/Implications: Our experimental CO_2 data and corresponding compositional model suggest that CO_2 solubility in ultramafic melts is significantly higher than basaltic melt at shallow MO conditions. As the MO cools, any C that is dissolved in the melt will precipitate out as graphite/diamond, and if convection is efficient, as the graphite is carried deeper it will redissolve into the MO. This process works in opposition to the 'carbon pump' hypothesis [1,2], meaning that as the shallow MO cools, it will degas CO_2 to the early atmosphere rather than trap it in the deeper mantle as a solid C phase for both Earth and Mars.

References: [1] Dasgupta (2013) *RiMG*, *75*, 183-229. [2] Hirschmann (2012) *EPSL*, *341*, 48-57. [3] Li et al. (2015) *EPSL*, *415*, 54-66. [4] Holloway et al. (1992) *EJM*, *4*, 105-114. [5] Brey (1976) *CMP*, *57*, 215-221. [6] Brooker et al. (2001) *CG*, *174*, 225-239. [7] Walter (1998) *JP*, *39*, 29-60. [8] O'Neill et al. (2006) *AM*, *91*, 404-412. [9] Hirschmann (2000) *G3*, *1*, 2000GC000070. [10] Zhang and Herzberg (1994) *JGR*, *99*, 17729-17742. [11] Matsukage et al. (2013) *JMPS*, *108*, 201-214. [12] Collinet et al. (2015) *EPSL*, *427*, 83-94.